

Robust Zinc(II)porphyrin Catalyst for Visible Light Induced C–H Arylation of Heteroarenes

Anu Janaagal, Sanyam, Anirban Mondal, and Iti Gupta*



Cite This: <https://doi.org/10.1021/acs.joc.3c00385>



Read Online

ACCESS |



Metrics & More

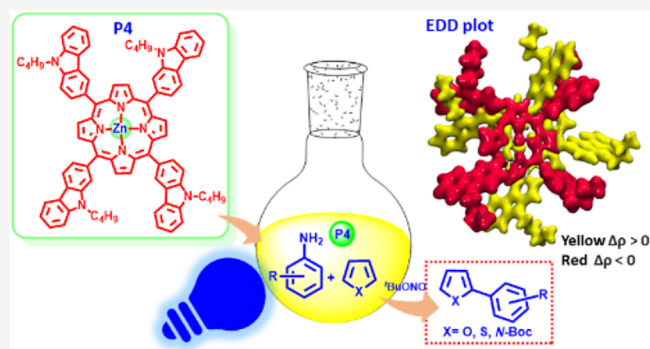


Article Recommendations



Supporting Information

ABSTRACT: Zinc(II)porphyrin catalyzed light induced C–H arylation of heteroarenes from anilines is discussed. The method is nontoxic and efficient, using only 0.5 mol % of porphyrin catalyst to produce bi(hetero)aryls in good yields. This work demonstrates the potential use of porphyrin photocatalysts as efficient and robust alternatives to organic dyes.



Photoredox catalysis is a rapidly growing area of chemical synthesis that uses visible light as its primary energy source.¹ During photoredox catalysis, a light absorbing dye (photocatalyst) can trap the photon energy and get activated,² which then induces an organic molecule/substrate to participate in a distinctive reaction pathway that may not be possible to achieve thermally.³ Photoredox catalysis is representative of sustainable and green chemistry, as it uses freely available, nonhazardous light energy and converts it into chemical energy.⁴ In the past few decades, photoredox catalysis has been used in various applications viz. CO₂ reduction, water splitting, dye sensitized solar cells (DSSCs), etc.⁵ It has been extensively used in different types of cross-coupling reactions to make C–X, C–C, C–O, C–S bonds and cycloaddition reactions.^{6–8} Seminal contributions from MacMillan and co-workers involve widespread usage of Ru(II) and Ir(III)-polypyridyl complexes as photocatalysts for C–C bond formation and C–H activation reactions.^{9,10} Similarly, Yoon's group has applied photoredox catalysis for cycloaddition reactions, whereas Stephenson and co-workers used it for natural product synthesis and reduction dehalogenation reactions.^{11,12}

Typically, after light irradiation a photoredox catalyst can undergo single electron transfer (SET) with the organic substrate or vice versa.¹³ A synergism between the electrochemical and photophysical properties of photoredox catalysts and substrates defines the criteria for selecting the correct photoredox catalyst.¹⁴ Based on electrochemical properties, the photoexcited catalyst (PC*) is accountable for the photo-induced electron transfer initiating a cycle by a reductive or oxidative quenching pathway.¹⁵ Ru(II) and Ir(III)polypyridyl complexes have been extensively explored in catalyzing organic

substrates (Chart S1).¹⁶ Due to the high cost and toxic nature of the heavy metal complexes, organic-dye-based catalysis is currently studied. Organic dyes like eosin Y are pH dependent and have ineffective reduction power.¹⁷ These limitations of metal complexes and organic dyes attract more attention toward utilizing macrocyclic complexes like porphyrins as photoredox catalysts.¹⁸ Porphyrin macrocycles are essential for survival, as they play major role in photosynthesis and oxygen transport.¹⁹ These macrocyclic complexes have the potential to undergo oxidation and reduction processes along with good absorption in the visible region, which makes these molecules more potent for photochemical reactions and photoredox catalysis. Features such as being nontoxic and biodegradable are the main advantages of these complexes. Due to their unique properties a variety of organic transformations, such as oxidations, reductions, epoxidation, carbon–carbon, and carbon–heteroatom bond formations, are routinely catalyzed by metalloporphyrins.²⁰

It has always been challenging to effectively build C–C bonds in a safe, affordable, and environmentally friendly manner. Due to the prevalence of bi(hetero)aryl structural motifs in organic materials, agrochemicals, and active medicinal components, their synthesis is one of the most significant transformations in organic chemistry.²¹ Direct C–H

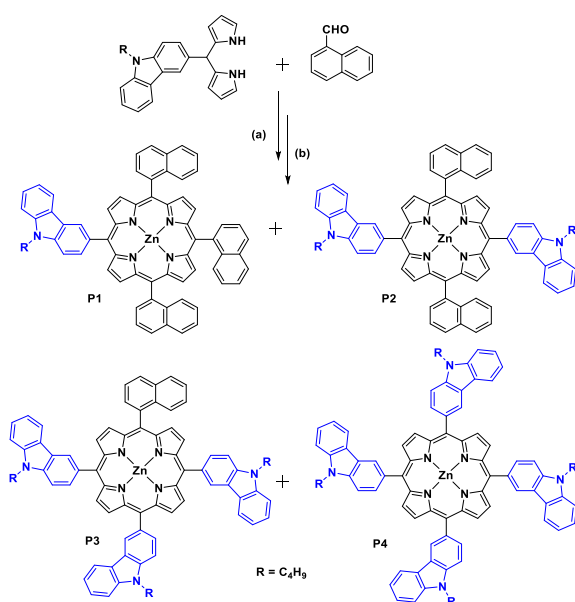
Received: February 20, 2023

arylation of heteroarenes has drawn much attention since it can avoid double preactivation required by both the substrates. Diazonium salts have been widely used in arylation processes because they contain a weak and labile C–N link in their structure.²² Since the 1930s, the copper-catalyzed version of this transition also known as the Meerwein arylation has been recognized, but still it has some significant limitations, including low yields and high catalyst loading.²³ There are various strategies reported in literature modifying the original synthetic method using thermal and photochemical reaction conditions.²⁴ König et al. reported eosin Y catalyzed direct arylation of heteroarenes, enol acetates, and alkenes with diazonium salts.²⁵ Ru(II) complexes and titanium oxide transition metal catalysts were used in photoredox catalysis for arylation reactions.²⁶ In 2016, Kadish and co-workers used free-base porphyrins and zinc-porphyrins as photoredox catalysts for the reaction of aldehydes with diazo compounds.²⁷ Later König and Gryko in a collaborative work demonstrated light-induced arylation of heteroarenes in moderate to good yields using diazonium salts as substrates.²⁸

Herein, we report an efficient and versatile method of C–H arylation of heteroarenes from anilines using 0.5 mol % of photoredox catalyst. The *meso*-heteroaryl substituted zinc porphyrins were synthesized and used as photocatalysts under visible light. The electrochemical, photophysical, and DFT studies were performed to demonstrate single electron transfer from a zinc porphyrin catalyst to the substrate during the course of C–H arylation of various heteroarenes.

The zinc porphyrins **P1**, **P2**, **P3**, and **P4** were synthesized by condensation of 1-naphthaldehyde and 9-butyl-3-(di(1*H*-pyrrol-2-yl)methyl)-9*H*-carbazole in two steps as shown in Scheme 1. The crude reaction mixture of free base porphyrins was passed through a silica gel column and treated with zinc acetate in a mixture of chloroform and methanol (2:1). After neutral alumina column chromatography, zinc porphyrins were

Scheme 1. Synthesis of Free Base Porphyrins and Their Zinc Complexes^a



^a(a) TFA, DCM, 5 h, followed by DDQ, 1 h, rt; (b) Zn(OAc)₂, MeOH:CHCl₃ (1:2), reflux.

characterized by ¹H NMR, ¹³C NMR, and HRMS (Figures S1–S12).

The absorption and emission studies of zinc porphyrins were carried out in toluene, and photophysical data are summarized in Tables S1 and S2. The comparative absorption and emission spectra are shown in the Figure S13. The zinc porphyrins exhibited one high energy Soret band and two lower energy Q bands, arising from the first excited state and vibrational overtones, respectively. The Soret band appeared around 429–435 nm, followed by Q bands in between 551 and 597 nm. The Soret bands of zinc porphyrins have molar absorption coefficients in the range 448,000–597,000 M⁻¹ cm⁻¹. A bathochromic shift is noticed upon changing the number of *meso*-*N*-butylcarbazolyl groups; this could be due to the shift of electron density from the carbazole rings to the porphyrin core. Also, the TD-DFT studies showed intramolecular charge transfer (ICT) from the *meso*-carbazole rings to the porphyrin core, which can be seen in HOMO–LUMO orbitals diagram of porphyrins **P1**–**P4** (Figures S93, S94). As compared to zinc tetraphenylporphyrin (ZnTPP), the Soret and Q-bands of **P4** porphyrin were red-shifted by 13 and 9 nm, respectively.²⁹ The zinc porphyrins **P1**–**P4** typically exhibited two emission bands with vibronic structures around 600–653 nm. The first and second emission bands of **P4** porphyrin showed red shifts of 16 and 8 nm, respectively with respect to those of ZnTPP.²⁹ The fluorescence quantum yields of porphyrins **P1**–**P4** were around 4% to 5%. The time-resolved fluorescence studies revealed the singlet state lifetime of **P1**–**P4** in between 1.5 and 2.2 ns (Figure S14, Table S1). The emission quantum yields and lifetime data are comparable with those of the standard ZnTPP.

For calculation of the excited state redox potential porphyrins **P1**–**P4**, the cyclic voltammetry studies were carried out in dry dichloromethane (Figures S15–S17). Porphyrins **P1**–**P4** showed typical reversible two-electron oxidation and reduction processes.³⁰ The redox potentials of porphyrins **P1**–**P4** were compared with ZnTPP (Table 1).³¹

Table 1. CV Data of Compounds Recorded in DCM

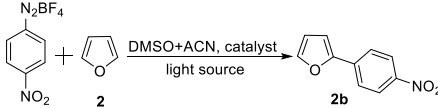
Porphyrin	$E_{1/2}(\text{ox})/\text{V vs SCE}$		$E_{1/2}(\text{red})/\text{V vs SCE}$	
	I	II	I	II
ZnTPP	0.80	1.09	-1.25	-1.65
P1	0.74	1.03	-1.62	-1.82
P2	0.69	0.98	-1.64	-1.83
P3	0.66	0.94	-1.66	-1.85
P4	0.60	0.86	-1.68	-1.88

Due to the presence of the electron donor group at *meso*-positions, porphyrins **P1**–**P4** were easily oxidized at lower potentials. For porphyrins **P1** and **P4**, the first oxidation potentials were anodically shifted by 0.06 and 0.2 V compared to ZnTPP (Figures S15–S16). The reduction potentials of **P1**–**P4** were shifted to more negative values, indicating that these porphyrins are difficult to reduce than ZnTPP (Figure S17). These porphyrins **P1**–**P4** with red-shifted emission bands, enhanced emission quantum yields, and lower oxidation potentials can be very good photoredox catalysts for organic reactions.

With this consideration, porphyrins **P1**–**P4** were screened for the C–H arylation reactions of heteroarenes. C–H bond arylation of heteroarenes with aryl diazonium salts was performed in the presence of a porphyrin catalyst under blue

light irradiation. Initially, different conditions were examined by choosing solvent, wavelength, catalyst, and catalyst loading at room temperature. During the primary studies, 4-bromoaniline and furan with **P4** as a photocatalyst was taken to check the impact of different solvents on product yields (Table S3). The reaction did not proceed in methanol and acetone solvents. In the case of ethanol, ethyl acetate, nitromethane, and dimethyl formamide, product yields were very poor. The mixture of dimethyl sulfoxide and acetonitrile afforded a better yield of the product, as compared to only acetonitrile or dimethyl sulfoxide (Table S3). To optimize the reaction conditions further, 4-nitrobenzenediazonium tetrafluoroborate and furan were used under blue light irradiation. Among all zinc porphyrins, **P4** assured product formation with maximum yields (Table 2, entries 1–4). Irradiation of the reaction

Table 2. Optimization of Reaction Conditions^a



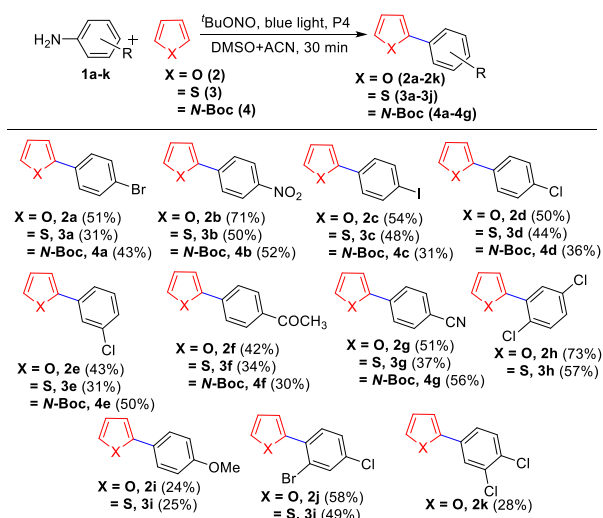
Entry	Catalyst	Light source	Catalyst loading (mol %)	Yield ^b (%)
1	P1	Blue	0.5	68
2	P2	Blue	0.5	62
3	P3	Blue	0.5	67
4	P4	Blue	0.5	70
5	P4	White	0.5	55
6	P4	Blue	0.75	56
7	P4	Blue	0.25	66
8	P4	Blue	0.1	63
9 ^c	P4	Blue	0.5	71

^aReaction conditions: 4-nitrobenzenediazonium tetrafluoroborate (0.30 mmol), furan (3.0 mmol), irradiation with light (24 W) for 30 min under N₂ atm at rt. ^bIsolated yields after purification. ^c4-Nitroaniline (0.30 mmol), furan (3.0 mmol), ^tBuONO (0.45 mmol).

mixture with white light resulted in low product yield (Table 2, entry 5). The reaction was performed with 0.1 to 0.75 mol % catalyst loading of **P4**, and the best yield was observed with 0.5 mol % of catalyst. As diazonium salts are very unstable and expensive, a test reaction was conducted to generate diazonium salt *in situ* using *tert*-butyl nitrite (Table 2, entry 9). No change in product yield was observed when diazonium salt was generated *in situ*, so for the remaining reactions, substituted anilines were taken as substrates.

Control experiments were performed by using diazonium salt, and only traces of the product were produced when reactions were performed without light or a catalyst. With the optimized conditions, other heteroarenes such as thiophene and *N*-Boc pyrrole were also explored for C–H arylation using blue light (Scheme 2). In the case of thiophene and *N*-Boc pyrrole, products were obtained in moderate to good yields. Arylation of heteroarenes was possible with both electron-rich and electron-deficient anilines. Different *ortho*-, *meta*-, and *para*-substituted anilines were tested for the C–H arylation. As per the previous report the diazonium salts having electron-withdrawing groups gave better product yields, than the electron-rich diazonium salts.³² No such trend is observed in the reactions catalyzed by zinc porphyrin **P4** reported in this work. Porphyrin **P4** successfully tolerated a variety of anilines containing different functional groups such as bromo, nitro, chloro, iodo, cyano, etc. Furthermore, the reaction of 2-methyl

Scheme 2. Scope of Arylation of Heteroarenes with Substituted Anilines^a



^aReaction conditions: aniline (0.3 mmol), heteroarene (3 mmol) furan, 1.5 mmol thiophene or 0.6 mmol *N*-Boc pyrrole, ^tBuONO (0.45 mmol) irradiation with light (24 W) for 30 min under N₂ atm at rt.

furan with substituted anilines were performed, and observed yields were between 9% and 33% (Scheme S1).

The density-functional theory (DFT) studies were carried out for porphyrins **P1**–**P4** (Figures S89–S92), and the optimized geometries displayed perpendicular orientations of the *meso*-naphthyl and *meso*-*N*-butylcarbazole rings with respect to the porphyrin plane. Time-dependent density-functional theory (TD-DFT) studies provided good agreement of the calculated absorption maxima with the observed Soret bands of the porphyrins (Table S4). The energy gap between the HOMO and LUMO of porphyrins **P1**–**P4** was found to be in the range 2.76 to 2.86 eV (Figures S93–S94). In the case of **P4** (Figure S94), it was observed that major transitions are taking place from HOMO–1 → LUMO and HOMO–5 → LUMO+1 with the maximum oscillatory strength of 0.44 and 0.35. It is challenging to demonstrate experimentally whether the electron transfer happens from the ground or the excited state. Furthermore, it is impossible to foresee whether a transition will occur from the singlet or triplet state. Theoretical results based on the calculated redox potentials and Δ*G* values indicated SET from the singlet excited state of **P4** to the aryl diazonium salts.³³

The reaction profile diagram (RPD) is used to explain SET and reaction mechanism (Figure 1). A proposed mechanism for C–H arylation of heteroarenes includes five steps. Initially, the diazonium salt is formed from aniline, and the **P4** porphyrin catalyst became excited by light irradiation. In the next step, single electron is transferred from the porphyrin ring to the diazonium salt, and a phenyl radical is generated, which is an energetically highly unfavorable process.

Further, a radical intermediate is produced by the addition of a phenyl radical and heteroarene. This radical is transformed into a carbocation intermediate by electron transfer to the porphyrin cation, which involves only a small amount of energy. In the final step, the product is formed, which is highly favorable (Figure 1). The free radical mechanism of C–H arylation of aryl diazonium salts is well documented.^{34,35} When

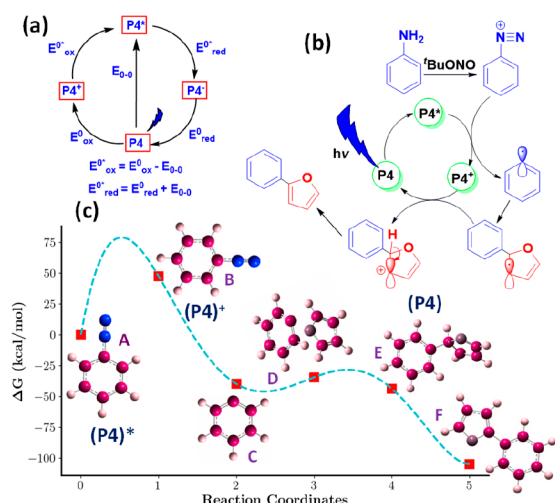
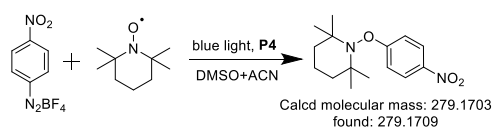


Figure 1. (a) Latimer diagram used to predict the excited-state redox potentials; (b) Plausible mechanism of reaction; (c) Computed reaction profile for C–H arylation of heteroarenes. (P4) ground state of catalyst. (P4)* excited state of catalyst. (P4)⁺ catalyst after SET.

TEMPO was added into the reaction of furan with nitro diazonium salt in the presence of P4, no product was observed as shown in Scheme 3. And HRMS mass was observed for the corresponding adduct (Figure S88), supporting the radical pathway.

Scheme 3. Experiment with TEMPO to Check the Radical Species



For the P4 porphyrin the ground state redox potential values are -0.96 and -1.34 V (Table S5) for the formation of cation and anion, respectively. The negative values reflect that the P4 porphyrin has a lower tendency to undergo the electron transfer process in the ground state. The DFT calculated excited state redox potentials of P4 in the singlet state are 1.15 and 0.77 V for the cation and anion, respectively. This indicated that the porphyrin can act as a better electron donor and acceptor in the excited state. The DFT estimated redox potentials for the cation formation from the singlet and triplet states are 1.15 and 0.21 V, respectively, which resulted in prominent electron transfer from the singlet state of P4 to the aryl diazonium salt. The charge distribution over the zinc porphyrin P4 is seen with the help of the Electron Density Difference (EDD) plot as shown in Figure S95. The cyan region of the plot showed the electron-dense area, while the purple region represented the electron-deficient part of the molecule. An EDD plot displayed the change in electron density of porphyrin from the excited state to the cationic form and supported SET from the catalyst P4.

In summary, four zinc porphyrins were synthesized and characterized by NMR and HRMS. An environment-friendly and sustainable approach for C–H arylation of heteroarenes was developed. The diazonium salts were generated *in situ*, and the same procedure persisted for many substrates. In addition to furan, thiophene and *N*-Boc pyrrole were also tested for

arylation reactions under blue light. Good agreement is observed between the experimental and DFT-calculated results. DFT studies suggested that an electron is transferred from the singlet excited state. Additionally, the DFT calculated redox potential values for P4 catalyst are similar to the experimental results. This work opens the door for the organic transformations catalyzed by porphyrin based photoredox systems. Porphyrin based photocatalysts are economical, efficient, and robust alternatives to the pH sensitive organic dyes or heavy metal-based catalysts.

EXPERIMENTAL SECTION

General Synthesis of Porphyrins. 9-Butyl-3-(di(1*H*-pyrrol-2-yl)methyl)-9*H*-carbazole has been synthesized as per literature reports.³⁶ In a 100 mL round-bottom flask, 9-butyl-3-(di(1*H*-pyrrol-2-yl)methyl)-9*H*-carbazole (513 mg, 1.4 mmol, 1.5 equiv) and α -naphthaldehyde (150 mg, 0.96 mmol, 1 equiv) were dissolved in 35 mL of dry DCM under N₂ atmosphere at room temperature. Trifluoroacetic acid (44 μ L, 0.57 mmol, 0.6 equiv) was added after 5 min, and the reaction mixture was left under continuous stirring in the dark. After 5 h, 2,3-dichloro-5,6-dicyano-1,4-benzoquinone (DDQ, 653 mg, 2.88 mmol, 3 equiv) was added, and the reaction mixture was left for another 1 h in the open air. Four porphyrin-like spots were observed on TLC, and for confirmation, UV-spectra were recorded. TEA (triethylamine, 50 μ L) was added, and then silica gel column chromatography was performed to remove excess DDQ. A freebase porphyrins mixture was dissolved in CHCl₃, and a Zn(OAc)₂ solution (10 equiv, dissolved in methanol) was added. The reaction was refluxed using an oil bath at 80 °C for 12–15 h. The reaction was monitored by TLC and UV–visible spectroscopy. The appearance of green color on silica TLC indicated the formation of zinc porphyrins. Zinc porphyrins were purified by neutral alumina column chromatography using DCM/hexane as a mobile phase.

Porphyrin P1. Magenta solid, mp > 250 °C. Yield 5% (33 mg). $R_f = 0.7$ (DCM/Hexane 3:7). IR (neat cm⁻¹): 3052, 2955, 2919, 2858, 1656, 1589, 1492, 1340, 1207. ¹H NMR (500 MHz, Chloroform-*d*): δ (in ppm) 8.94–8.89 (m, 3H), 8.67–8.64 (m, 2H), 8.58–8.54 (m, 4H), 8.31–8.23 (m, 7H), 8.12–8.09 (m, 4H), 7.86–7.80 (m, 3H), 7.70 (d, $J = 8, 1$ H), 7.55 (t, $J = 8.5, 2$ H), 7.46 (t, $J = 7.5, 3$ H), 7.23–7.11 (m, 7H), 4.54 (t, $J = 7$ Hz, 2H), 2.11–2.05 (m, 2H), 1.62 (m, 2H), 1.07 (t, $J = 7.5$ Hz, 3H). ¹³C{¹H} NMR (125 MHz, Chloroform-*d*): δ (in ppm) 151.08, 151.03, 150.9, 150.79, 150.74, 141.2, 140.07, 140.01, 136.88, 136.80, 133.2, 132.8, 132.7, 132.5, 132.4, 132.1, 132.0, 131.9, 131.6, 128.8, 128.3, 127.7, 126.0, 125.8, 124.1, 122.8, 122.6, 121.3, 120.6, 119.0, 118.6, 118.0, 108.9, 106.4, 43.2, 31.3, 20.7, 14.0. HRMS [ESI]: C₆₆H₄₆N₅Zn⁺ [M + H]⁺: calcd m/z 972.3039, found 972.3034.

Porphyrin P2. Magenta solid, mp > 250 °C. Yield 16% (172 mg). $R_f = 0.6$ (DCM/Hexane 3:7). IR (neat cm⁻¹): 3046, 2955, 2913, 2846, 1583, 1468, 1334, 1207. ¹H NMR (500 MHz, Chloroform-*d*): δ (in ppm) 8.99 (s, 1H), 8.91–8.88 (m, 5H), 8.91–8.63 (m, 3H), 8.56 (s, 1H), 8.36–8.24 (m, 6H), 8.16–8.10 (m, 4H), 7.88–7.82 (m, 2H), 7.70 (t, $J = 8.5$ Hz, 2H), 7.5 (m, 4H), 7.46 (t, $J = 7$ Hz, 2H), 7.29–7.26 (m, 1H), 7.10–7.06 (m, 5H), 4.53 (t, $J = 7$ Hz, 4H), 2.10–2.06 (m, 4H), 1.64–1.61 (m, 4H), 1.07 (t, $J = 7.5$ Hz, 6H). ¹³C{¹H} NMR (125 MHz, Chloroform-*d*): δ (in ppm) 151.0, 150.7, 141.3, 140.2, 140.0, 136.9, 136.8, 133.3, 132.8, 132.5, 132.4, 132.2, 131.9, 131.8, 131.6, 131.5, 128.8, 128.3, 127.7, 126.3, 126.0, 125.8, 125.5, 124.1, 123.3, 122.8, 122.5, 121.3, 120.6, 119.0, 118.5, 118.2, 108.9, 106.4, 43.2, 31.4, 20.7, 14.0. HRMS [ESI]: C₇₂H₅₅N₆Zn⁺ [M + H]⁺: calcd m/z 1067.3774, found 1067.3766.

Porphyrin P3. Magenta solid, mp > 250 °C. Yield 9% (109 mg). $R_f = 0.4$ (DCM/Hexane 3:7). IR (neat cm⁻¹): 3046, 2955, 2931, 2858, 1602, 1462, 1334, 1213. ¹H NMR (500 MHz, Chloroform-*d*): δ (in ppm) 8.99–8.91 (m, 10H), 8.66 (m, 2H), 8.37–8.12 (m, 11H), 7.86 (t, $J = 8.5$ Hz, 1H), 7.72 (t, $J = 9.5$ Hz, 3H), 7.56–7.45 (m, 8H), 7.10 (s, 1H), 4.54 (t, $J = 7.5$ Hz, 6H), 2.12–2.06 (m, 6H), 1.64–1.58 (m, 6H), 1.08 (t, $J = 7$ Hz, 9H). ¹³C{¹H} NMR (125 MHz, Chloroform-

d): δ (in ppm) 151.1, 150.9, 150.8, 141.2, 140.3, 139.9, 136.9, 133.4, 132.8, 132.5, 132.4, 132.2, 132.1, 131.5, 128.9, 128.3, 127.7, 126.3, 126.0, 125.8, 125.5, 124.1, 122.9, 122.5, 122.0, 121.3, 120.6, 119.0, 117.9, 108.9, 106.4, 43.2, 31.4, 20.8, 14.0. HRMS [ESI]: $C_{78}H_{63}N_7Zn^+$ [M]⁺: calcd m/z 1161.4431, found 1161.4434.

Porphyrin P4. Magenta solid, mp > 250 °C. Yield 6% (53 mg). R_f = 0.3 (DCM/Hexane 3:7). IR (neat cm^{-1}): 3046, 2955, 2919, 2846, 1595, 1468, 1330, 1213. ¹H NMR (500 MHz, dimethyl sulfoxide- d_6): δ (in ppm) 8.97 (s, 2H), 8.94 (s, 2H), 8.81 (s, 8H), 8.34–8.28 (m, 8H), 7.96 (t, J = 8 Hz, 4H), 7.76 (d, J = 8.5 Hz, 4H), 7.54 (t, J = 7.5 Hz, 4H), 7.23 (t, J = 7.5 Hz, 4H), 4.63 (t, J = 6.5 Hz, 8H), 2.05–1.95 (m, 8H), 1.55–1.51 (m, 8H), 1.02 (t, J = 7 Hz, 12H). ¹³C{¹H} NMR (125 MHz, dimethyl sulfoxide- d_6): δ (in ppm) 150.5, 141.4, 139.8, 133.9, 132.7, 132.2, 126.5, 122.6, 121.6, 121.1, 119.3, 109.9, 107.4, 31.5, 29.4, 20.5, 14.3. HRMS [ESI]: $C_{84}H_{72}N_8Zn^+$ [M]⁺: calcd m/z 1256.5166, found 1256.5178.

Photoredox Reaction. The diazonium salt/aniline (0.3 mmol, 1 equiv) and heteroarene (3 mmol furan, 3 mmol 2-methylfuran, 1.5 mmol thiophene or 0.6 mmol *N*-Boc pyrrole) was taken in 10 mL round-bottom borosilicate glass flask. Solvent (600 μ L) and catalyst (1.8 mg, 1.5×10^{-3} mmol, 0.5 mol %) were added to it, followed by addition of *tert*-butyl nitrite. The reaction mixture was stirred at room temperature and irradiated by Smartchem Synth Photoreactor (24 W blue LED, 440 nm). The products were purified by silica gel column chromatography using ethyl acetate/hexane mixture as eluent. After column chromatography products were confirmed by ¹H and ¹³C NMR (Figure S18–S87).

2-(4-Bromophenyl)furan (2a).²¹ White solid, mp 93–95 °C. Yield 51% (34 mg). ¹H NMR (500 MHz, Chloroform- d): δ (in ppm) 7.54–7.47 (m, 5H), 6.65 (d, J = 3.5 Hz, 1H), 6.47–6.46 (m, 1H), ¹³C{¹H} NMR (125 MHz, Chloroform- d): δ (in ppm) 152.9, 142.4, 131.8, 129.8, 125.3, 121.0, 111.8, 105.5.

2-(4-Nitrophenyl)furan (2b).²¹ Yellow solid, mp 145–147 °C. Yield 71% (40.5 mg). ¹H NMR (500 MHz, Chloroform- d): δ (in ppm) 8.25 (d, J = 9 Hz, 2H), 7.80 (d, J = 9 Hz, 2H), 7.57 (s, 1H), 6.88 (d, J = 3.5 Hz, 1H), 6.56–6.55 (m, 1H). ¹³C{¹H} NMR (125 MHz, Chloroform- d): δ (in ppm) 151.7, 146.4, 144.1, 136.4, 124.3, 123.9, 112.4, 108.9.

2-(4-Iodophenyl)furan (2c).²⁸ White solid, mp 112–114 °C. Yield 54% (44 mg). ¹H NMR (500 MHz, Chloroform- d): δ (in ppm) 7.70 (d, J = 8.5 Hz, 2H), 7.47 (s, 1H), 7.40 (d, J = 9 Hz, 2H), 6.66 (d, J = 2.5 Hz, 1H), 6.47–6.46 (m, 1H). ¹³C{¹H} NMR (125 MHz, Chloroform- d): δ (in ppm) 153.0, 142.4, 137.7, 130.3, 125.4, 111.8, 105.6, 92.4.

2-(4-Chlorophenyl)furan (2d).²¹ Yellow solid, mp 72–75 °C. Yield 50% (24 mg). ¹H NMR (500 MHz, Chloroform- d): δ (in ppm) 7.59 (d, J = 8.5 Hz, 2H), 7.47 (s, 1H), 7.34 (d, J = 8.5 Hz, 2H), 6.62 (d, J = 3 Hz, 1H), 6.48–6.47 (m, 1H). ¹³C{¹H} NMR (125 MHz, Chloroform- d): δ (in ppm) 152.9, 142.3, 132.9, 129.3, 128.8, 125.0, 111.7, 105.4.

2-(3-Chlorophenyl)furan (2e).^{37a} Colorless viscous liquid. Yield 43% (23 mg). ¹H NMR (500 MHz, Chloroform- d): δ (in ppm) 7.65 (s, 1H), 7.53 (d, J = 8 Hz, 1H), 7.47 (s, 1H), 7.29 (t, J = 8 Hz, 1H), 7.22–7.20 (m, 1H), 6.66 (d, J = 3.5 Hz, 1H), 6.48–6.47 (m, 1H). ¹³C{¹H} NMR (125 MHz, Chloroform- d): δ (in ppm) 152.5, 142.6, 134.7, 132.5, 129.9, 127.2, 123.8, 121.8, 111.8, 106.0.

1-(4-(Furan-2-yl)phenyl)ethan-1-one (2f).^{37b} White solid, mp 117–120 °C. Yield 42% (23.5 mg). ¹H NMR (500 MHz, Chloroform- d): δ (in ppm) 7.98 (d, J = 9 Hz, 2H), 7.74 (d, J = 8.5 Hz, 2H), 7.53 (s, 1H), 6.80 (d, J = 3.5 Hz, 1H), 6.52–6.51 (m, 1H), 2.61 (s, 3H). ¹³C{¹H} NMR (125 MHz, Chloroform- d): δ (in ppm) 197.4, 152.8, 143.3, 135.5, 134.9, 128.9, 123.5, 112.1, 107.4, 26.5.

4-(Furan-2-yl)benzotrile (2g).²¹ White solid, mp 76–78 °C. Yield 51% (26 mg). ¹H NMR (500 MHz, Chloroform- d): δ (in ppm) 7.74 (d, J = 9 Hz, 2H), 7.65 (d, J = 8.5 Hz, 2H), 7.54 (s, 1H), 6.81 (d, J = 3.5 Hz, 1H), 6.53–6.52 (m, 1H). ¹³C{¹H} NMR (125 MHz, Chloroform- d): δ (in ppm) 152.0, 143.7, 134.6, 132.6, 123.9, 118.9, 112.2, 110.3, 108.1.

2-(2,5-Dichlorophenyl)furan (2h). Colorless viscous liquid. Yield 73% (46.8 mg). ¹H NMR (500 MHz, Chloroform- d): δ (in ppm) 7.86 (s, 1H), 7.52 (s, 1H), 7.35 (d, J = 8.5 Hz, 1H), 7.19–7.14 (m, 2H), 6.54–6.53 (m, 1H). ¹³C{¹H} NMR (125 MHz, Chloroform- d): δ (in ppm) 148.9, 142.6, 132.9, 131.8, 130.4, 128.0, 127.7, 127.4, 111.9, 111.8. HRMS [ESI]: $C_{10}H_7Cl_2O^+$ [M + H]⁺: calcd m/z 212.9896, found 212.9870.

2-(4-Methoxyphenyl)furan (2i).²¹ White solid, mp 72–75 °C. Yield 24% (12.7 mg). ¹H NMR (500 MHz, Chloroform- d): δ (in ppm) 7.60 (d, J = 9 Hz, 2H), 7.42 (s, 1H), 6.92 (d, J = 9 Hz, 2H), 6.51 (d, J = 3.5 Hz, 1H), 6.45–6.44 (m, 1H), 3.83 (s, 3H). ¹³C{¹H} NMR (125 MHz, Chloroform- d): δ (in ppm) 159.0, 154.0, 141.3, 125.2, 124.0, 114.1, 111.5, 103.3, 55.3.

2-(2-Bromo-4-chlorophenyl)furan (2j).^{37c} Colorless viscous liquid. Yield 58% (45 mg). ¹H NMR (500 MHz, Chloroform- d): δ (in ppm) 7.73 (d, J = 8.5 Hz, 1H), 7.66 (s, 1H), 7.51 (s, 1H), 7.35–7.32 (m, 1H), 7.17 (d, J = 3.5 Hz, 1H), 6.53–6.52 (m, 1H). ¹³C{¹H} NMR (125 MHz, Chloroform- d): δ (in ppm) 150.3, 142.4, 133.6, 133.2, 129.8, 129.3, 127.7, 119.6, 111.5, 110.9.

2-(3,4-Dichlorophenyl)furan (2k).^{37a} Colorless viscous liquid. Yield 28% (18 mg). ¹H NMR (500 MHz, Chloroform- d): δ (in ppm) 7.74 (s, 1H), 7.48–7.46 (m, 2H), 7.44 (s, 1H), 6.66 (d, J = 3 Hz, 1H), 6.48–6.47 (m, 1H). ¹³C{¹H} NMR (125 MHz, Chloroform- d): δ (in ppm) 151.6, 142.8, 132.9, 130.9, 130.7, 130.6, 125.5, 122.9, 111.9, 106.4.

2-(4-Bromophenyl)thiophene (3a).²⁸ Colorless viscous liquid. Yield 31% (22.3 mg). ¹H NMR (500 MHz, Chloroform- d): δ (in ppm) 7.50–7.46 (m, 4H), 7.29 (d, J = 4 Hz, 2H), 7.09–7.07 (m, 1H). ¹³C{¹H} NMR (125 MHz, Chloroform- d): δ (in ppm) 143.1, 133.3, 131.9, 128.1, 127.4, 125.2, 123.5, 121.2.

2-(4-Nitrophenyl)thiophene (3b).²¹ Yellow solid, mp 145–147 °C. Yield 50% (31 mg). ¹H NMR (500 MHz, Chloroform- d): δ (in ppm) 8.24 (d, J = 9 Hz, 2H), 7.74 (d, J = 9 Hz, 2H), 7.48–7.44 (m, 2H), 7.16–7.14 (m, 1H). ¹³C{¹H} NMR (125 MHz, Chloroform- d): δ (in ppm) 146.6, 141.6, 140.6, 128.7, 127.6, 126.0, 125.7, 124.4.

2-(4-Iodophenyl)thiophene (3c).^{37d} Colorless viscous liquid. Yield 48% (41 mg). ¹H NMR (500 MHz, Chloroform- d): δ (in ppm) 7.69 (d, J = 8.5 Hz, 2H), 7.34 (d, J = 8.5 Hz, 2H), 7.30–7.29 (m, 2H), 7.08–7.06 (m, 1H). ¹³C{¹H} NMR (125 MHz, Chloroform- d): δ (in ppm) 143.1, 137.9, 133.9, 128.1, 127.6, 125.3, 123.5, 92.6. HRMS [ESI]: $C_{10}H_8IS^+$ [M + H]⁺: calcd m/z 286.9386, found 286.9366.

2-(4-Chlorophenyl)thiophene (3d).^{37e} White solid, mp 91–93 °C. Yield 44% (25.8 mg). ¹H NMR (500 MHz, Chloroform- d): δ (in ppm) 7.53 (d, J = 8.5 Hz, 2H), 7.33 (d, J = 9 Hz, 2H), 7.29–7.28 (m, 2H), 7.08–7.07 (m, 1H). ¹³C{¹H} NMR (125 MHz, Chloroform- d): δ (in ppm) 143.1, 133.2, 132.9, 129.0, 128.1, 127.6, 127.1, 125.2, 123.4.

2-(3-Chlorophenyl)thiophene (3e).^{37f} Colorless viscous liquid. Yield 31% (18.3 mg). ¹H NMR (500 MHz, Chloroform- d): δ (in ppm) 7.59 (s, 1H), 7.49–7.47 (m, 1H), 7.37–7.30 (m, 4H), 7.09–7.08 (m, 1H). ¹³C{¹H} NMR (125 MHz, Chloroform- d): δ (in ppm) 142.7, 136.1, 134.7, 130.1, 128.1, 127.3, 125.8, 125.5, 124.0, 123.8.

1-(4-(Thiophen-2-yl)phenyl)ethan-1-one (3f).^{37b} White solid, mp 125–127 °C. Yield 34% (20.7 mg). ¹H NMR (500 MHz, Chloroform- d): δ (in ppm) 7.97 (d, J = 7.5 Hz, 2H), 7.70 (d, J = 8.5 Hz, 2H), 7.43 (d, J = 3.5 Hz, 1H), 7.37 (d, J = 5 Hz, 1H), 7.13–7.11 (m, 1H), 2.61 (s, 3H). ¹³C{¹H} NMR (125 MHz, Chloroform- d): δ (in ppm) 197.3, 142.9, 138.8, 135.7, 129.1, 128.3, 126.4, 125.6, 124.6, 26.6.

4-(Thiophen-2-yl)benzotrile (3g).²¹ White solid, mp 105–107 °C. Yield 37% (20.6 mg). ¹H NMR (500 MHz, Chloroform- d): δ (in ppm) 7.70 (d, J = 8.5 Hz, 2H), 7.65 (d, J = 8.5 Hz, 2H), 7.43–7.40 (m, 2H), 7.14–7.12 (m, 1H). ¹³C{¹H} NMR (125 MHz, Chloroform- d): δ (in ppm) 142.0, 138.6, 132.7, 128.5, 127.0, 126.1, 125.1, 118.8, 110.5.

2-(2,5-Dichlorophenyl)thiophene (3h). Colorless viscous liquid. Yield 57% (39.4 mg). ¹H NMR (500 MHz, Chloroform- d): δ (in ppm) 7.52 (s, 1H), 7.42–7.36 (m, 3H), 7.22–7.20 (m, 1H), 7.12–7.10 (m, 1H). ¹³C{¹H} NMR (125 MHz, Chloroform- d): δ (in ppm)

138.7, 134.6, 132.6, 131.5, 131.0, 128.4, 128.2, 127.2, 126.2. HRMS [ESI]: $C_{10}H_7Cl_2S^+ [M + H]^+$: calcd m/z 228.9640, found 228.9641.

2-(4-Methoxyphenyl)thiophene (3i).^{37b} Colorless viscous liquid. Yield 25% (14.3 mg). ¹H NMR (500 MHz, Chloroform-*d*): δ (in ppm) 7.53 (d, $J = 9$ Hz, 2H), 7.21–7.19 (m, 2H), 7.06–7.04 (m, 1H), 6.91 (d, $J = 8.5$ Hz, 2H), 3.83 (s, 3H). ¹³C{¹H} NMR (125 MHz, Chloroform-*d*): δ (in ppm) 159.1, 144.3, 127.9, 127.5, 127.4, 123.8, 122.0, 114.2, 55.3.

2-(2-Bromo-4-chlorophenyl)thiophene (3j).^{37c} Colorless viscous liquid. Yield 49% (40 mg). ¹H NMR (500 MHz, Chloroform-*d*): δ (in ppm) 7.69 (s, 1H), 7.41–7.39 (m, 2H), 7.32–7.27 (m, 2H), 7.11–7.10 (m, 1H). ¹³C{¹H} NMR (125 MHz, Chloroform-*d*): δ (in ppm) 140.5, 134.1, 133.9, 133.2, 132.5, 128.0, 127.6, 127.0, 126.4, 123.1.

tert-Butyl 2-(4-bromophenyl)-1H-pyrrole-1-carboxylate (4a).^{37g} Colorless viscous liquid. Yield 43% (42 mg). ¹H NMR (500 MHz, Chloroform-*d*): δ (in ppm) 7.37–7.36 (m, 1H), 7.33 (s, 1H), 7.27 (t, $J = 5.5$ Hz, 2H), 7.23–7.21 (m, 1H), 6.22 (t, $J = 3.5$ Hz, 1H), 6.21–6.20 (m, 1H), 1.37 (s, 9H). ¹³C{¹H} NMR (125 MHz, Chloroform-*d*): δ (in ppm) 149.2, 136.1, 133.37, 133.31, 129.3, 128.8, 127.2, 127.1, 123.0, 115.0, 112.9, 110.6, 83.9, 27.6.

tert-Butyl 2-(4-nitrophenyl)-1H-pyrrole-1-carboxylate (4b).²¹ Yellow solid, mp 134–136 °C. Yield 52% (45 mg). ¹H NMR (500 MHz, Chloroform-*d*): δ (in ppm) 8.21 (d, $J = 9$ Hz, 2H), 7.51 (d, $J = 9$ Hz, 2H), 7.41–7.40 (m, 1H), 6.33–6.32 (m, 1H), 7.28–7.26 (t, $J = 7$, 1H), 1.43 (s, 9H). ¹³C{¹H} NMR (125 MHz, Chloroform-*d*): δ (in ppm) 148.9, 146.6, 140.7, 132.7, 129.5, 124.3, 122.9, 116.2, 111.1, 84.5, 27.7.

tert-Butyl 2-(4-iodophenyl)-1H-pyrrole-1-carboxylate (4c).^{37g} Colorless viscous liquid. Yield 31% (34 mg). ¹H NMR (500 MHz, Chloroform-*d*): δ (in ppm) 7.67 (d, $J = 8$ Hz, 2H), 7.34–7.33 (m, 1H), 7.09 (d, $J = 8$ Hz, 1H), 6.22–6.21 (t, $J = 6.5$ Hz, 1H), 6.18–6.17 (m, 1H), 1.40 (s, 9H). ¹³C{¹H} NMR (125 MHz, Chloroform-*d*): δ (in ppm) 149.1, 136.6, 133.89, 133.84, 130.9, 122.9, 114.8, 110.7, 92.7, 83.9, 27.6.

tert-Butyl 2-(4-chlorophenyl)-1H-pyrrole-1-carboxylate (4d).^{37g} Colorless viscous liquid. Yield 36% (30 mg). ¹H NMR (500 MHz, Chloroform-*d*): δ (in ppm) 7.35–7.26 (m, 5H), 6.22 (t, $J = 3.5$ Hz, 1H), 6.18–6.17 (m, 1H), 1.39 (s, 9H). ¹³C{¹H} NMR (125 MHz, Chloroform-*d*): δ (in ppm) 149.1, 133.7, 133.1, 132.8, 130.4, 130.0, 128.0, 127.0, 122.8, 114.7, 110.6, 83.8, 27.6.

tert-Butyl 2-(3-chlorophenyl)-1H-pyrrole-1-carboxylate (4e).^{37h} Yellow viscous liquid. Yield 50% (41.5 mg). ¹H NMR (500 MHz, Chloroform-*d*): δ (in ppm) 7.37–7.36 (m, 1H), 7.33 (s, 1H), 7.27 (d, $J = 5$ Hz, 2H), 7.24–7.21 (m, 1H), 6.23–6.20 (m, 2H), 1.37 (s, 9H). ¹³C{¹H} NMR (125 MHz, Chloroform-*d*): δ (in ppm) 149.2, 136.1, 133.36, 133.30, 129.3, 128.8, 127.2, 127.1, 123.0, 114.9, 110.6, 83.9, 27.6. HRMS [ESI]: $C_{15}H_{17}ClNO_2^+ [M + H]^+$: calcd m/z 278.0942, found 278.0938.

tert-Butyl 2-(4-acetylphenyl)-1H-pyrrole-1-carboxylate (4f).³⁷ⁱ Colorless viscous liquid. Yield 30% (26 mg). ¹H NMR (500 MHz, Chloroform-*d*): δ (in ppm) 7.95 (d, $J = 8.5$ Hz, 2H), 7.44 (d, $J = 3.5$ Hz, 2H), 7.38–7.37 (m, 1H), 6.27–6.24 (m, 2H), 2.61 (s, 3H), 1.3 (s, 9H). ¹³C{¹H} NMR (125 MHz, Chloroform-*d*): δ (in ppm) 197.7, 149.1, 139.0, 135.5, 133.9, 129.0, 127.7, 123.6, 115.5, 110.9, 84.1, 27.6, 26.4.

tert-Butyl 2-(4-cyanophenyl)-1H-pyrrole-1-carboxylate (4g).²¹ Colorless viscous liquid. Yield 56% (45 mg). ¹H NMR (500 MHz, Chloroform-*d*): δ (in ppm) 8.22 (d, $J = 9$ Hz, 2H), 7.51 (d, $J = 9$ Hz, 2H), 7.41–7.40 (m, 1H), 6.33–6.32 (m, 1H), 6.28–6.26 (t, $J = 3.5$, 1H), 1.43 (s, 9H). ¹³C{¹H} NMR (125 MHz, Chloroform-*d*): δ (in ppm) 148.9, 146.6, 140.7, 132.7, 129.5, 124.3, 122.9, 116.5, 111.1, 84.5, 27.7.

2-Methyl-5-(4-nitrophenyl)furan (5a).^{37j} Yellow solid, mp 128–130 °C. Yield 18% (11 mg). ¹H NMR (500 MHz, Chloroform-*d*): δ (in ppm) 8.22 (d, $J = 9$ Hz, 2H), 7.73 (d, $J = 9$ Hz, 2H), 6.78 (d, $J = 3$ Hz, 1H), 6.15–6.14 (m, 1H), 2.41 (s, 3H). ¹³C{¹H} NMR (125 MHz, Chloroform-*d*): δ (in ppm) 154.6, 150.1, 136.7, 124.3, 123.2, 110.2, 108.8, 13.8.

2-(4-Iodophenyl)-5-methylfuran (5b).^{37k} Yellow solid, mp 84–86 °C. Yield 9% (8 mg). ¹H NMR (500 MHz, Chloroform-*d*): δ (in

ppm) 7.66 (d, $J = 9$ Hz, 2H), 7.35 (d, $J = 8.5$ Hz, 2H), 6.55 (d, $J = 3$ Hz, 1H), 6.05 (t, $J = 3$ Hz, 1H), 2.35 (s, 3H). ¹³C{¹H} NMR (125 MHz, Chloroform-*d*): δ (in ppm) 152.4, 151.2, 137.6, 130.6, 124.9, 107.9, 106.6, 91.5, 13.7.

1-(4-(5-Methylfuran-2-yl)phenyl)ethan-1-one (5c).^{37j} Yellow solid, mp 112–114 °C. Yield 27% (16.2 mg). ¹H NMR (500 MHz, Chloroform-*d*): δ (in ppm) 7.95 (d, $J = 8$ Hz, 2H), 7.69 (d, $J = 9$ Hz, 2H), 6.70 (d, $J = 3$ Hz, 1H), 6.11–6.10 (m, 1H), 2.60 (s, 3H), 2.39 (s, 3H). ¹³C{¹H} NMR (125 MHz, Chloroform-*d*): δ (in ppm) 197.4, 153.5, 151.1, 135.2, 135.0, 128.9, 122.9, 108.6, 108.3, 26.5, 13.8.

4-(5-Methylfuran-2-yl)benzonitrile (5d).^{37j} Yellow solid, mp 110–112 °C. Yield 33% (18 mg). ¹H NMR (500 MHz, Chloroform-*d*): δ (in ppm) 7.68 (d, $J = 8.5$ Hz, 2H), 7.62 (d, $J = 8.5$ Hz, 2H), 6.70 (d, $J = 3.5$ Hz, 1H), 6.12–6.11 (m, 1H), 2.39 (s, 3H). ¹³C{¹H} NMR (125 MHz, Chloroform-*d*): δ (in ppm) 154.0, 150.3, 134.9, 132.5, 123.3, 119.1, 109.5, 109.3, 108.5, 13.8.

2-(2-Bromo-4-chlorophenyl)-5-methylfuran (5e).^{37c} White solid, mp 61–63 °C. Yield 23% (19 mg). ¹H NMR (500 MHz, Chloroform-*d*): δ (in ppm) 7.72 (d, $J = 8.5$ Hz, 1H), 7.49 (d, $J = 2$ Hz, 1H), 7.31–7.29 (m, 1H), 7.09 (d, $J = 3$ Hz, 1H), 6.119–6.112 (m, 1H), 2.36 (s, 3H). ¹³C{¹H} NMR (125 MHz, Chloroform-*d*): δ (in ppm) 152.5, 148.6, 133.5, 132.5, 129.9, 128.7, 127.6, 119.0, 112.1, 107.8, 13.6.

ASSOCIATED CONTENT

Data Availability Statement

The data underlying this study are available in the published article and its Supporting Information.

Supporting Information

The Supporting Information is available free of charge at <https://pubs.acs.org/doi/10.1021/acs.joc.3c00385>.

The spectral characterization data including photo-physical and electrochemical studies are available. Also, DFT calculations data are provided (PDF)

AUTHOR INFORMATION

Corresponding Author

Iti Gupta – Indian Institute of Technology Gandhinagar, Gandhinagar, Gujarat 382055, India; orcid.org/0000-0003-4288-8661; Email: iti@iitgn.ac.in

Authors

Anu Janaagal – Indian Institute of Technology Gandhinagar, Gandhinagar, Gujarat 382055, India

Sanyam – Indian Institute of Technology Gandhinagar, Gandhinagar, Gujarat 382055, India

Anirban Mondal – Indian Institute of Technology Gandhinagar, Gandhinagar, Gujarat 382055, India

Complete contact information is available at:

<https://pubs.acs.org/doi/10.1021/acs.joc.3c00385>

Notes

The authors declare no competing financial interest.

ACKNOWLEDGMENTS

Financial support from IIT Gandhinagar and SERB-POWER, Govt. of India (Grant No: SPG/2021/004023) is greatly acknowledged. A.J. is grateful to IIT Gandhinagar for a fellowship. Sanyam thanks the Council of Scientific and Industrial Research (CSIR), India, for a fellowship. A.M. acknowledges IITGN and PARAM Ananta for the computational facility.

REFERENCES

- (1) (a) König, B. Photocatalysis in organic synthesis—past, present, and future. *Eur. J. Org. Chem.* **2017**, 2017, 1979–1981. (b) Zeitler, K. Photoredox catalysis with visible light. *Angew. Chem., Int. Ed.* **2009**, *48*, 9785–9789. (c) Srivastava, V.; Singh, P. K.; Singh, P. P. Recent Advances of Visible-Light Photocatalysis in the Functionalization of Organic Compounds. *J. Photochem. Photobiol. C* **2022**, *50*, 100488.
- (2) Romero, N. A.; Nicewicz, D. A. Organic Photoredox Catalysis. *Chem. Rev.* **2016**, *116*, 10075–10166.
- (3) Reckenthäler, M.; Griesbeck, A. G. Photoredox Catalysis for Organic Syntheses. *Adv. Synth. Catal.* **2013**, *355*, 2727–2744.
- (4) Twilton, J.; Le, C. C.; Zhang, P.; Shaw, M. H.; Evans, R. W.; MacMillan, D. W. C. The Merger of Transition Metal and Photocatalysis. *Nat. Rev. Chem.* **2017**, *1*, 0052.
- (5) (a) Takeda, H.; Ishitani, O. Development of Efficient Photocatalytic Systems for CO₂ Reduction Using Mononuclear and Multinuclear Metal Complexes Based on Mechanistic Studies. *Coord. Chem. Rev.* **2010**, *254*, 346–354. (b) Graetzel, M. Artificial photosynthesis: water cleavage into hydrogen and oxygen by visible light. *Acc. Chem. Res.* **1981**, *14*, 376–384. (c) Kalyanasundaram, K.; Grätzel, M. Applications of Functionalized Transition Metal Complexes in Photonic and Optoelectronic Devices. *Coord. Chem. Rev.* **1998**, *177*, 347–414.
- (6) (a) Ghosh, I.; Marzo, L.; Das, A.; Shaikh, R.; König, B. Visible Light Mediated Photoredox Catalytic Arylation Reactions. *Acc. Chem. Res.* **2016**, *49*, 1566–1577. (b) Tellis, J. C.; Primer, D. N.; Molander, G. A. Single-electron transmetalation in organoboron cross-coupling by photoredox/nickel dual catalysis. *Science* **2014**, *345*, 433–436. (c) Lévêque, C.; Chenneberg, L.; Corcé, V.; Goddard, J. P.; Ollivier, C.; Fensterbank, L. Primary Alkyl Bis-Catecholato Silicates in Dual Photoredox/Nickel Catalysis: Aryl- and Heteroaryl-Alkyl Cross Coupling Reactions. *Org. Chem. Front.* **2016**, *3*, 462–465. (d) Jouffroy, M.; Primer, D. N.; Molander, G. A. Base-Free Photoredox/Nickel Dual-Catalytic Cross-Coupling of Ammonium Alkylsilicates. *J. Am. Chem. Soc.* **2016**, *138*, 475–478. (e) Johnston, C. P.; Smith, R. T.; Allmendinger, S.; MacMillan, D. W. C. Metallaphotoredox-Catalysed sp³-sp³ Cross-Coupling of Carboxylic Acids with Alkyl Halides. *Nature* **2016**, *536*, 322–325.
- (7) (a) Majek, M.; von Wangelin, A. J. Organocatalytic Visible Light Mediated Synthesis of Aryl Sulfides. *Chem. Commun.* **2013**, *49*, 5507–5509. (b) Terrett, J. A.; Cuthbertson, J. D.; Shurtleff, V. W.; MacMillan, D. W. C. Switching on Elusive Organometallic Mechanisms with Photoredox Catalysis. *Nature* **2015**, *524*, 330–334.
- (8) Yoon, T. P. Photochemical Stereocontrol Using Tandem Photoredox-Chiral Lewis Acid Catalysis. *Acc. Chem. Res.* **2016**, *49*, 2307–2315.
- (9) Millet, A.; Cesana, P. T.; Sedillo, K.; Bird, M. J.; Schlau-Cohen, G. S.; Doyle, A. G.; Macmillan, D. W. C.; Scholes, G. D. Bioinspired Supercharging of Photoredox Catalysis for Applications in Energy and Chemical Manufacturing. *Acc. Chem. Res.* **2022**, *55*, 1423–1434.
- (10) Chan, A. Y.; Perry, I. B.; Bissonnette, N. B.; Buksh, B. F.; Edwards, G. A.; Frye, L. I.; Garry, O. L.; Lavagnino, M. N.; Li, B. X.; Liang, Y.; Mao, E.; Millet, A.; Oakley, J. V.; Reed, N. L.; Sakai, H. A.; Seath, C. P.; MacMillan, D. W. C. Metallaphotoredox: The Merger of Photoredox and Transition Metal Catalysis. *Chem. Rev.* **2022**, *122*, 1485–1542.
- (11) Ischay, M. A.; Anzovino, M. E.; Du, J.; Yoon, T. P. Efficient Visible Light Photocatalysis of [2 + 2] Enone Cycloadditions. *J. Am. Chem. Soc.* **2008**, *130*, 12886–12887.
- (12) (a) Kárkás, M. D.; Porco, J. A.; Stephenson, C. R. J. Photochemical Approaches to Complex Chemotypes: Applications in Natural Product Synthesis. *Chem. Rev.* **2016**, *116*, 9683–9747. (b) Narayanam, J. M. R.; Stephenson, C. R. J. Visible Light Photoredox Catalysis: Applications in Organic Synthesis. *Chem. Soc. Rev.* **2011**, *40*, 102–113. (c) Narayanam, J. M. R.; Tucker, J. W.; Stephenson, C. R. J. Electron-Transfer Photoredox Catalysis: Development of a Tin-Free Reductive Dehalogenation Reaction. *J. Am. Chem. Soc.* **2009**, *131*, 8756–8757. (d) Allen, A. R.; Noten, E. A.; Stephenson, C. R. J. Aryl Transfer Strategies Mediated by Photo-induced Electron Transfer. *Chem. Rev.* **2022**, *122*, 2695–2751. (e) Romero, K. J.; Galliher, M. S.; Pratt, D. A.; Stephenson, C. R. J. Radicals in Natural Product Synthesis. *Chem. Soc. Rev.* **2018**, *47*, 7851–7866.
- (13) (a) Shaw, M. H.; Twilton, J.; MacMillan, D. W. C. Photoredox Catalysis in Organic Chemistry. *J. Org. Chem.* **2016**, *81*, 6898–6926. (b) Ravelli, D.; Pratti, S.; Fagnoni, M. Carbon-Carbon Bond Forming Reactions via Photogenerated Intermediates. *Chem. Rev.* **2016**, *116*, 9850–9913.
- (14) (a) Tay, N. E. S.; Lehnher, D.; Rovis, T. Photons or Electrons? A Critical Comparison of Electrochemistry and Photoredox Catalysis for Organic Synthesis. *Chem. Rev.* **2022**, *122*, 2487–2649. (b) Pitre, S. P.; McTiernan, C. D.; Scaiano, J. C. Understanding the kinetics and spectroscopy of photoredox catalysis and transition-metal-free alternatives. *Acc. Chem. Res.* **2016**, *49*, 1320–1330. (c) Goliszewska, K.; Rybicka-Jasińska, K.; Clark, J. A.; Vullev, V. I.; Gryko, D. Photoredox catalysis: the reaction mechanism can adjust to electronic properties of a catalyst. *ACS Catal.* **2020**, *10*, 5920–5927.
- (15) Majek, M.; Jacobi Von Wangelin, A. Mechanistic Perspectives on Organic Photoredox Catalysis for Aromatic Substitutions. *Acc. Chem. Res.* **2016**, *49*, 2316–2327.
- (16) Prier, C. K.; Rankic, D. A.; MacMillan, D. W. C. Visible Light Photoredox Catalysis with Transition Metal Complexes: Applications in Organic Synthesis. *Chem. Rev.* **2013**, *113*, 5322–5363.
- (17) (a) Majek, M.; Filace, F.; von Wangelin, A. J. On the mechanism of photocatalytic reactions with eosin Y. *Beilstein J. Org. Chem.* **2014**, *10*, 981–989. (b) Herbrük, F.; Camarero González, P.; Krstic, M.; Puglisi, A.; Benaglia, M.; Sanz, M. A.; Rossi, S. Eosin Y: Homogeneous Photocatalytic In-Flow Reactions and Solid-Supported Catalysts for In-Batch Synthetic Transformations. *Appl. Sci.* **2020**, *10*, 5596.
- (18) (a) De Souza, A. A. N.; Silva, N. S.; Müller, A. V.; Polo, A. S.; Brocksom, T. J.; de Oliveira, K. T. Porphyrins as Photoredox Catalysts in Csp²-H Arylations: Batch and Continuous Flow Approaches. *J. Org. Chem.* **2018**, *83*, 15077–15086. (b) Capaldo, L.; Ertl, M.; Fagnoni, M.; Knör, G.; Ravelli, D. Antimony-Oxo Porphyrins as Photocatalysts for Redox-Neutral C-H to C-C Bond Conversion. *ACS Catal.* **2020**, *10*, 9057–9064.
- (19) Kadish, K. M.; Royal, G.; Van Caemelbecke, E.; Gueletti, L. In *The Porphyrin Handbook*; Kadish, K. M., Smith, K. M., Guillard, R., Eds.; Academic Press: Boston, 2000; Vol. 9, pp 1–220.
- (20) (a) Costa e Silva, R.; da Silva, L. O.; de Andrade Bartolomeu, A.; Brocksom, T. J.; de Oliveira, K. T. Recent Applications of Porphyrins as Photocatalysts in Organic Synthesis: Batch and Continuous Flow Approaches. *Beilstein J. Org. Chem.* **2020**, *16*, 917–955. (b) Mandal, T.; Das, S.; De Sarkar, S. Nickel (II) Tetraphenylporphyrin as an efficient photocatalyst featuring visible light promoted dual redox activities. *Adv. Synth. Catal.* **2019**, *361*, 3200–9. (c) Pandey, V.; Janaagal, A.; Jain, M.; Mori, S.; Gupta, I. A₂B₂ type porphyrins with meso-donor groups: Synthesis, X-ray structures, DFT studies and photocatalytic application using sunlight. *Dyes Pigm.* **2023**, *209*, 110861. (d) Janaagal, A.; Pandey, V.; Sabharwal, S.; Gupta, I. meso-Carbazole substituted palladium porphyrins: Efficient catalysts for visible light induced oxidation of aldehydes. *J. Porphyr. Phthalocyanines* **2021**, *25*, 571–581. (e) Pandey, V.; Jain, D.; Pareek, N.; Gupta, I. Pd(II) porphyrins: Synthesis, singlet oxygen generation and photoassisted oxidation of aldehydes to carboxylic acids. *Inorg. Chim. Acta* **2020**, *502*, 119339.
- (21) Shiro, T.; Fukaya, T.; Tobe, M. The Chemistry and Biological Activity of Heterocycle-Fused Quinolinone Derivatives: A Review. *Eur. J. Med. Chem.* **2015**, *97*, 397–408.
- (22) (a) Allongue, P.; Delamar, M.; Desbat, B.; Fagebaume, O.; Hitmi, R.; Pinson, J.; Savéant, J.-M. Covalent Modification of Carbon Surfaces by Aryl Radicals Generated from the Electrochemical Reduction of Diazonium Salts. *J. Am. Chem. Soc.* **1997**, *119*, 201–207. (b) Galli, C. Radical Reactions of Arenediazonium Ions: An Easy Entry into the Chemistry of the Aryl Radical. *Chem. Rev.* **1988**, *88*, 765–792.

- (23) Meerwein, H.; Büchner, E.; van Emster, K. *J. Prakt. Chem.* **1939**, *152*, 237.
- (24) (a) Hari, D. P.; König, B. The Photocatalyzed Meerwein Arylation: Classic Reaction of Aryl Diazonium Salts in a New Light. *Angew. Chem., Int. Ed.* **2013**, *52*, 4734–4743. (b) Hari, D. P.; Hering, T.; König, B. The Photoredox-Catalyzed Meerwein Addition Reaction: Intermolecular Amino-Arylation of Alkenes. *Angew. Chem., Int. Ed.* **2014**, *53*, 725–728. (c) Chen, H.; Nanayakkara, C. E.; Grassian, V. H. Titanium Dioxide Photocatalysis in Atmospheric Chemistry. *Chem. Rev.* **2012**, *112*, 5919–5948.
- (25) Hari, D. P.; Schroll, P.; König, B. Metal-Free, Visible-Light-Mediated Direct C-H Arylation of Heteroarenes with Aryl Diazonium Salts. *J. Am. Chem. Soc.* **2012**, *134*, 2958–2961.
- (26) (a) Gauchot, V.; Sutherland, D. R.; Lee, A. L. Dual Gold and Photoredox Catalyzed C-H Activation of Arenes for Aryl-Aryl Cross Couplings. *Chem. Sci.* **2017**, *8*, 2885–2889. (b) Zoller, J.; Fabry, D. C.; Rueping, M. Unexpected Dual Role of Titanium Dioxide in the Visible Light Heterogeneous Catalyzed C-H Arylation of Heteroarenes. *ACS Catal.* **2015**, *5*, 3900–3904.
- (27) Rybicka-Jasińska, K.; Shan, W.; Zawada, K.; Kadish, K. M.; Gryko, D. Porphyrins as photoredox catalysts: Experimental and theoretical studies. *J. Am. Chem. Soc.* **2016**, *138*, 15451–15458.
- (28) Rybicka-Jasińska, K.; König, B.; Gryko, D. Porphyrin-Catalyzed Photochemical C-H Arylation of Heteroarenes. *Eur. J. Org. Chem.* **2017**, *2017*, 2104–2107.
- (29) (a) Gouterman, M. In *The Porphyrins*; Dolphin, D., Ed.; Academic Press: New York, 1978; Vol. 3, pp 1–165. (b) Tobita, S.; Kaizu, Y.; Kobayashi, H.; Tanaka, I. Study of higher excited singlet states of zinc (II)-tetraphenylporphyrin. *J. Chem. Phys.* **1984**, *81*, 2962–2969. (c) Taniguchi, M.; Lindsey, J. S.; Bocian, D. F.; Holten, D. Comprehensive review of photophysical parameters (ϵ , Φ_f , τ_s) of tetraphenylporphyrin (H₂TPP) and zinc tetraphenylporphyrin (ZnTPP)—Critical benchmark molecules in photochemistry and photosynthesis. *J. Photochem. Photobiol.* **2021**, *46*, 100401. (d) Das, S.; Gupta, I. Synthetic aspects of carbazole containing porphyrins and porphyrinoids. *J. Porphyr. Phthalocyanines* **2019**, *23*, 367–409. (e) Kesavan, P. E.; Pandey, V.; Ishida, M.; Furuta, H.; Mori, S.; Gupta, I. Synthesis, photophysical properties and computational studies of beta-substituted porphyrin dyads. *Chem.—Asian J.* **2020**, *15*, 2015–2028.
- (30) (a) Kadish, K. M.; Morrison, M. M. Solvent and substituent effects on the redox reactions of para-substituted tetraphenylporphyrin. *J. Am. Chem. Soc.* **1976**, *98*, 3326–3328. (b) Kadish, K. M.; Van Caemelbecke, E. Electrochemistry of porphyrins and related macrocycles. *J. Solid State Electrochem.* **2003**, *7*, 254–258. (c) Das, S.; Bhat, H. R.; Balsukuri, N.; Jha, P. C.; Hisamune, Y.; Ishida, M.; Furuta, H.; Mori, S.; Gupta, I. Donor–acceptor type A₂B₂ porphyrins: synthesis, energy transfer, computational and electrochemical studies. *Inorg. Chem. Front.* **2017**, *4*, 618–638.
- (31) Bhyrappa, P.; Sankar, M.; Varghese, B. Mixed substituted porphyrins: structural and electrochemical redox properties. *Inorg. Chem.* **2006**, *45*, 4136–4149.
- (32) (a) Guo, Z.; Liu, X.; Che, Y.; Chen, D.; Xing, H. One-Pot Dual Catalysis of a Photoactive Coordination Polymer and Palladium Acetate for the Highly Efficient Cross-Coupling Reaction via Interfacial Electron Transfer. *Inorg. Chem.* **2022**, *61*, 2695–2705. (b) Wang, L.; Byun, J.; Li, R.; Huang, W.; Zhang, K. A. I. Molecular Design of Donor-Acceptor-Type Organic Photocatalysts for Metal-Free Aromatic C–C Bond Formations under Visible Light. *Adv. Synth. Catal.* **2018**, *360*, 4312–4318.
- (33) Demissie, T. B.; Ruud, K.; Hansen, J. H. DFT as a powerful predictive tool in photoredox catalysis: redox potentials and mechanistic analysis. *Organometallics* **2015**, *34*, 4218–4228.
- (34) Tatunashvili, E.; Chan, B.; Nashar, P. E.; McErlean, C. S. P. σ -Bond Initiated Generation of Aryl Radicals from Aryl Diazonium Salts. *Org. Biomol. Chem.* **2020**, *18*, 1812–1819.
- (35) (a) Zhang, S.; Tang, Z.; Bao, W.; Li, J.; Guo, B.; Huang, S.; Zhang, Y.; Rao, Y. Perylenequinonoid-Catalyzed Photoredox Activation for the Direct Arylation of (Het)Arenes with Sunlight. *Org. Biomol. Chem.* **2019**, *17*, 4364–4369. (b) Cai, X.; Liu, H.; Zhi, L.; Wen, H.; Yu, A.; Li, L.; Chen, F.; Wang, B. A G-C₃N₄/RGO Nanocomposite as a Highly Efficient Metal-Free Photocatalyst for Direct C-H Arylation under Visible Light Irradiation. *RSC Adv.* **2017**, *7*, 46132–46138.
- (36) Wang, H.; Chen, G.; Xu, X.; Chen, H.; Ji, S. *Dyes Pigm.* **2010**, *86*, 238–248.
- (37) (a) Hwang, E.; Lee, S. M.; Bak, S.; Hwang, H. M.; Kim, H.; Lee, H. Facile CH arylation using catalytically active terminal sulfurs of 2 dimensional molybdenum disulfide. *Tetrahedron Lett.* **2018**, *59*, 3969–3973. (b) Crespi, S.; Protti, S.; Fagnoni, M. Wavelength selective generation of aryl radicals and aryl cations for metal-free photoarylations. *J. Org. Chem.* **2016**, *81*, 9612–9619. (c) Gowrisankar, S.; Seayad, J. AgONO-Assisted Direct C-H Arylation of Heteroarenes with Anilines. *Chem.—Eur. J.* **2014**, *20*, 12754–12758. (d) Eroglu, Z.; Ozer, M. S.; Kubanaliev, T.; Kilic, H.; Metin, Ö. Synergism between few-layer black phosphorus and graphitic carbon nitride enhances the photoredox C–H arylation under visible light irradiation. *Catal. Sci. Technol.* **2022**, *12*, 5379–5389. (e) Monzón, D. M.; Santos, T.; Pinacho-Crisóstomo, F.; Martín, V. S.; Carrillo, R. Mild-Base-Promoted Arylation of (Hetero) Arenes with Anilines. *Chem.—Asian J.* **2018**, *13*, 325–333. (f) Cantillo, D.; Mateos, C.; Rincon, J. A.; de Frutos, O.; Kappe, C. O.; Light-Induced, C-H. Arylation of (Hetero) arenes by In Situ Generated Diazo Anhydrides. *Chem.—Eur. J.* **2015**, *21*, 12894–12898. (g) Kumar, M.; Sharma, S.; Sil, P.; Kushwaha, M.; Mayor, S.; Vishwakarma, R. A.; Singh, P. P. C–H Arylation of N-Heteroarenes under Metal-Free Conditions and its Application towards the Synthesis of Pentabromo-and Pentachloropseudilins. *Eur. J. Org. Chem.* **2019**, *2019*, 3591–3598. (h) Lee, P. H. Synthesis of 4, 4-Difluoro-4-bora-3a, 4a-diaza-s-indacene Dyes Bearing New Aryl Substituents at C3- and C5-Positions. *Bull. Korean Chem. Soc.* **2008**, *29*, 261–264. (i) Buglioni, L.; Riente, P.; Palomares, E.; Pericàs, M. A. Visible-light-promoted arylation reactions photocatalyzed by bismuth (III) oxide. *Eur. J. Org. Chem.* **2017**, *2017*, 6986–6990. (j) Song, A. X.; Zeng, X. X.; Ma, B. B.; Xu, C.; Liu, F. S. Direct (hetero) arylation of heteroarenes catalyzed by unsymmetrical Pd-PEPPSI-NHC complexes under mild conditions. *Organometallics* **2020**, *39*, 3524–3534. (k) Skhiri, A.; Beladhría, A.; Yuan, K.; Soulé, J. F.; Ben Salem, R.; Doucet, H. Pd-Catalyzed Direct Arylation of Heteroaromatics Using (Poly) halobenzenesulfonyl Chlorides as Coupling Partners: One Step Access to (Poly) halo-Substituted Bi(hetero) aryls. *Eur. J. Org. Chem.* **2015**, *2015*, 4428–4436.